

# White Matter Microstructural Integrity in Youth With Type 1 Diabetes

Jo Ann V. Antenor-Dorsey,<sup>1</sup> Erin Meyer,<sup>2</sup> Jerrel Rutlin,<sup>1</sup> Dana C. Perantie,<sup>1</sup> Neil H. White,<sup>4</sup> Ana Maria Arbelaez,<sup>4</sup> Joshua S. Shimony,<sup>3</sup> and Tamara Hershey<sup>1,2,3</sup>

Decreased white and gray matter volumes have been reported in youth with type 1 diabetes mellitus (T1DM), but the effects of hyperglycemia on white matter integrity have not been quantitatively assessed during brain development. We performed diffusion tensor imaging, using two complimentary approaches—region-of-interest and voxelwise tract-based spatial statistics—to quantify white matter integrity in a large retrospective study of T1DM youth and control participants. Exposure to chronic hyperglycemia, severe hyperglycemic episodes, and severe hypoglycemia, as defined in the Diabetes Control and Complications Trial (DCCT), were estimated through medical records review, HbA<sub>1c</sub> levels, and interview of parents and youth. We found lower fractional anisotropy in the superior parietal lobule and reduced mean diffusivity in the thalamus in the T1DM group. A history of three or more severe hyperglycemic episodes was associated with reduced anisotropy and increased diffusivity in the superior parietal lobule and increased diffusivity in the hippocampus. These results add microstructural integrity of white matter to the range of structural brain alterations seen in T1DM youth and suggest vulnerability of the superior parietal lobule, hippocampus, and thalamus to glycemic extremes during brain development. Longitudinal analyses will be necessary to determine how these alterations change with age or additional glycemic exposure. *Diabetes* 62:581–589, 2013

**T**he effects of type 1 diabetes mellitus (T1DM) on the central nervous system, especially during brain development, are controversial and not well understood. Structural magnetic resonance imaging (MRI) studies have found regional gray and white matter volume differences between youth with T1DM and control subjects (1,2), relating some of these findings to previous hypoglycemia or hyperglycemia exposure (3,4). These data and studies in adults have suggested a preferential vulnerability of some brain regions to diabetes and glycemic extremes. For example, we have found that white matter volume in the superior parietal region was decreased in youth with T1DM with greater hyperglycemic exposure (4), similar to findings in adults (5,6). Furthermore, studies of youth with T1DM have reported an association between

severe hypoglycemia and reduced (7) or increased hippocampal volumes (8). Volume estimates, however, do not assess the structural integrity of white matter tracts. Animal and some human studies have suggested that hyperglycemia (9,10) and hypoglycemia have been associated with changes in white matter microstructural integrity peripherally (11), but prior studies in youth with T1DM have not specifically examined the microstructural integrity of white matter tracts within the brain.

Diffusion tensor imaging (DTI) can be used to assess white matter microstructural integrity through the measurement of water molecule movement. DTI is sensitive to subtle white matter brain injury in humans (12) and can detect changes even when standard T2-weighted images appear normal and the white matter region volumes are similar (13). In addition, DTI measures have been directly validated by means of comparison with immunohistochemical indicators of axonal injury in animal models (14). In the current study, we examined DTI parameters using complementary region-of-interest (ROI)-based and voxelwise tract-based spatial statistics (TBSS) approaches to determine whether abnormalities in white matter microstructure are present in youth with T1DM and varying degrees of hyperglycemia or hypoglycemia exposure.

## RESEARCH DESIGN AND METHODS

**Subjects.** Youth aged 9–22 years with T1DM and nondiabetic siblings (healthy control subjects) were recruited from the Pediatric Diabetes Clinic at Washington University in St. Louis and St. Louis Children's Hospital. T1DM subjects were all seen by a pediatric endocrinologist at Washington University. Once a clinic member determined which patients met our basic inclusion and exclusion criteria (e.g., age, diagnoses), the families were referred to our research team for further discussion about the study. After reviewing the study demands and the more detailed exclusion criteria with the families, if interested, parents and children were consented and assented and then enrolled in the study. Subjects were excluded for mental retardation, chronic diseases other than T1DM (e.g., including hypothyroidism), significant neurologic history not due to diabetes, diagnosed psychiatric disorder, current use of psychoactive medications, known premature birth (<36 weeks' gestation) with complications, or contraindications to MRI (e.g., metal implants). T1DM participants were on insulin therapy for at least 2 years before study entry. Handedness was assessed with a modified Edinburgh Handedness Inventory. Procedures were approved by the Washington University School of Medicine Human Studies Committee, and all participants and their parents or guardians signed informed consents. Although some data from this cohort have been published previously (4,8,15,16), the white matter microstructural integrity analyses reported here have not been published previously except in abstract form.

**Clinical variables.** Detailed information about each diabetic participant's history of severe hypoglycemia, hyperglycemia, and other diabetes complications was collected by parental and child interview and medical record review. As defined in the Diabetes Control and Complications Trial (DCCT) (17), severe hypoglycemia was identified as an event with neurologic dysfunction, including seizure, loss of consciousness, and/or inability to arouse from sleep, that required assistance of someone other than the patient for treatment and improved after the administration of carbohydrate or glucagon injection (18). Severe hyperglycemia was identified as events including vomiting, ketosis evident in serum or urine, with or without acidemia, that required assistance of someone other than the patient for treatment and improved after

From the <sup>1</sup>Department of Psychiatry, Washington University School of Medicine, St. Louis, Missouri; the <sup>2</sup>Department of Neurology, Washington University School of Medicine, St. Louis, Missouri; the <sup>3</sup>Department of Radiology, Washington University School of Medicine, St. Louis, Missouri; and the <sup>4</sup>Department of Pediatrics, Washington University School of Medicine, St. Louis, Missouri.

Corresponding authors: Tamara Hershey, tammy@wustl.edu, and Jo Ann V. Antenor-Dorsey, joann@wustl.edu.

Received 25 May 2012 and accepted 25 July 2012.

DOI: 10.2337/db12-0696

© 2013 by the American Diabetes Association. Readers may use this article as long as the work is properly cited, the use is educational and not for profit, and the work is not altered. See <http://creativecommons.org/licenses/by-nc-nd/3.0/> for details.

See accompanying commentary, p. 341.

administration of insulin and/or intravenous fluids (Table 1). The number of severe hypoglycemic and hyperglycemic events was categorized zero (0 group), one to two (1–2 group), and three or more (3+ group) episodes because these variables were not normally distributed. Hyperglycemic exposure history was estimated from all available HbA<sub>1c</sub> test results. HbA<sub>1c</sub> tests approximated average blood glucose control over the previous 2–3 months. The amount of time represented by the HbA<sub>1c</sub> tests (HbA<sub>1c</sub> coverage) was calculated by multiplying the number of tests by 3 months and dividing by duration of diabetes in months (4). Participants with HbA<sub>1c</sub> coverage for <30% of their duration of diabetes (*n* = 10) were excluded from hyperglycemia analyses. Less-than-complete coverage was due to clinical appointments >3 months apart, transfers from other clinics, or use of total glycated hemoglobin tests instead of HbA<sub>1c</sub>.

To account for duration of exposure to hyperglycemia, a hyperglycemia exposure score was calculated. Because a child with an average HbA<sub>1c</sub> of 8% and duration of diabetes for 10 years has had more exposure to hyperglycemia than a child with the same average HbA<sub>1c</sub> for 2 years, a score that weighted duration and HbA<sub>1c</sub> equally was calculated by adding each patient's *z* score of median HbA<sub>1c</sub> to the *z* score of duration of diabetes. This method of calculation results in a near-normal distribution of scores, with higher scores indicating more overall exposure to hyperglycemia and lower scores, less. Thus, each child's hyperglycemia exposure score can be interpreted relative to this sample only. Blood glucose at the time of the MRI scan was also recorded and had to be above 70 mg/dL before beginning scanning.

**Image acquisition.** Structural images were acquired for each subject on a Siemens Sonata 1.5 Tesla imaging system with a standard Siemens 30-cm circularly polarized radio frequency head coil. Three to five images, consisting of 128 contiguous 1.25-mm sagittal slices, were acquired for each subject using magnetization-prepared rapid gradient echo (repetition time = 1,900 ms, echo time = 3.93 ms, flip angle = 15°, matrix = 256 × 256 pixels, voxel resolution = 1 × 1 × 1.25 mm, time = 7:07 min). Subjects with movement or other artifact were excluded from further analyses. Images with suspected anatomic abnormalities were referred to a neuroradiologist for review. Three subjects in the T1DM group were excluded for confirmed brain abnormalities: one had a pineal cyst, one had an arterial malformation in the medulla, and the other had hippocampal dysplasia that was severe enough to prevent the scan from aligning well with the brain atlas used for our structural analyses.

Diffusion-weighted images were collected to measure white matter microstructural integrity. We collected three sets of interleaved diffusion-weighted images (2-mm slice thickness, 12 directions at b values of 800, 1000 and 1200 s/mm<sup>2</sup> and a b = 0, transverse acquisition; repetition time = 4500, echo time = 80, voxel resolution = 2 × 2 × 2 mm, time = 1:26 × 18 = 25:48 min).

**Image processing.** The diffusion-weighted images were registered to the T2 (b = 0), which was registered to the best magnetization-prepared rapid gradient echo, which in turn was registered to an in-house atlas. Parametric maps were generated for mean diffusivity (which indicates the average magnitude of water molecule movement in the three axes), fractional anisotropy (which indicates the directionality of water molecule movement), and eigen values ( $\lambda_1$ ,  $\lambda_2$ , and  $\lambda_3$ ). Also recorded were the measures of axial diffusivity ( $\lambda_1$ ), which indicates the magnitude of water molecule movement along the principal axis, and

radial diffusivity [ $(\lambda_2 + \lambda_3)/2$ ], which indicates the average magnitude of water molecule movement in the two minor axes. Diffusion encodings corrupted by subject motion were automatically removed, and a residual map was created to determine the variance in the reconstructed data. A red-green-blue map was also used for quality control of parametric maps.

**Imaging analysis approach.** We analyzed FA, mean diffusivity, axial diffusivity, and radial diffusivity measures using two complementary methods 1) ROI-based approach and 2) voxelwise analysis using TBSS. The ROI method has several advantages over voxelwise analyses: it minimizes the risk of type 1 error, avoids the many statistical assumptions over voxelwise analyses, and allows for tailoring ROIs to avoid partial volume effects, thus reducing the effect of imperfect registration procedures (12). However, voxelwise analyses consider all of the imaging space without regard for arbitrary or unreliable boundaries and without a priori assumptions. We used both approaches here to provide a comprehensive view of the white matter microstructural abnormalities in T1DM youth.

**ROI method:** Regions were selected based on a well-established DTI atlas (19) and were checked by a neuroradiologist with expertise in DTI. We then compared the placement of the regions on each subject's red-green-blue map, T1, and T2 images simultaneously. ROIs were shifted by a few voxels as necessary by a trained technician to better conform to each individual's native anatomy. Finalized regions were then applied to each subject's fractional anisotropy, mean diffusivity, axial diffusivity, and radial diffusivity parametric maps and sampled using Analyze 8.0 software (20). Raters have established interrater correlation coefficients above 0.90 for fractional diffusivity and mean diffusivity values for all ROIs. To minimize false-positives, we focused on a select number of regions: 2 a priori regions (superior parietal lobule and hippocampus) and 10 exploratory regions (cerebellum, optic radiation, posterior limb of the internal capsule, corpus callosum (splenium, body and genu), centrum semiovale, thalamus, putamen, and pons), and averaged values from left and right homologous regions (Fig. 1). **TBSS.** As a complementary approach, we used TBSS (21) voxelwise analyses to confirm our ROI findings and to explore white matter effects in other locations without regard for strict anatomical boundaries. Diffusion weighted images were internally motion-corrected using nine-parameter affine (rigid body + scanner axis stretch) registration using software developed in-house. Then, BET (FMRIB Brain Extraction Tool) was used to compute a brain mask from each individual's motion-corrected, aligned, and averaged DWI data set, and FDT (FMRIB diffusion toolbox) was used to compute fractional anisotropy maps.

To create a target template for registration, a subset was chosen from the entire subject pool to provide an even distribution of males and females and ages. Fractional anisotropy images in the target group were then nonlinearly aligned to 1- × 1- × 1-mm space and to each other. The target image was the image that required the least amount of warping for all other fractional anisotropy images to align to it. All fractional anisotropy images in the entire subject pool were then nonlinearly aligned to each other in 1- × 1- × 1-mm space and to the target image. The target image was affine-aligned into MNI152 standard space, and every fractional anisotropy image was then transformed into 1- × 1- × 1-mm MNI152 space. A mean fractional anisotropy image was calculated and used to produce the mean fractional anisotropy skeleton to represent the center of white matter tracts. Fractional anisotropy images were projected onto the mean fractional anisotropy skeleton and thresholded set at fractional anisotropy = 0.2 for voxelwise analyses. Mean diffusivity, axial diffusivity, and radial diffusivity images were also calculated.

**Statistical analyses.** For all ROI analyses, we performed univariate analyses of each region with group (T1DM vs. control) or subgroup (severe hyperglycemia or severe hypoglycemia subgroups) as the independent variable and covarying age and sex. The hyperglycemia exposure score was correlated with DTI measures for each region. The criteria for significance was *P* < 0.05 for our two a priori regions and *P* < 0.005 (Bonferroni correction, 0.05/10 regions) for our exploratory regions within analyses for each DTI parameter (fractional anisotropy, mean diffusivity, axial diffusivity, and radial diffusivity). Regions that survived multiple comparisons corrections were examined for differences between groups with post hoc comparisons.

For voxelwise analyses, DTI parameter images were analyzed using Randomize (FSL, FMRIB, Oxford, U.K.), a permutation-based multiple comparisons corrected statistical approach (22). Age and sex were covaried in analyses comparing groups, as described for the ROI analyses. Each analysis used the software-specific multiple comparison correction procedures.

**RESULTS**

**T1DM versus control subjects**

**Demographic and clinical data.** The study included 73 T1DM youth and 30 healthy control subjects. T1DM and control groups were similar in all demographic measures, with the exception that there were proportionally more right-handed youth in the control than in the T1DM group

TABLE 1  
Symptoms reported during severe hyperglycemic episodes

Symptoms	Of 63 severe hyperglycemic episodes reported
	(%)
Ketonuria	86
Vomiting	70
Tired	41
Weakness	38
Drowsiness	30
Dizziness	27
Irritable	27
Sweating	27
Headaches	24
Confused	22
Pallor	21
Other*	<20

\*Trouble moving body, slurred speech, poor concentration, stomach pain, aggressive, tearful, trembling, disoriented, dehydrated, hungry, disoriented, flu, strange thoughts, thirsty, unresponsive, loss of consciousness, problems breathing, clammy, hyperventilation, loss of appetite, muscle ache, nausea, blurred vision, cold, lethargic, sluggish, stubborn, stumbling.

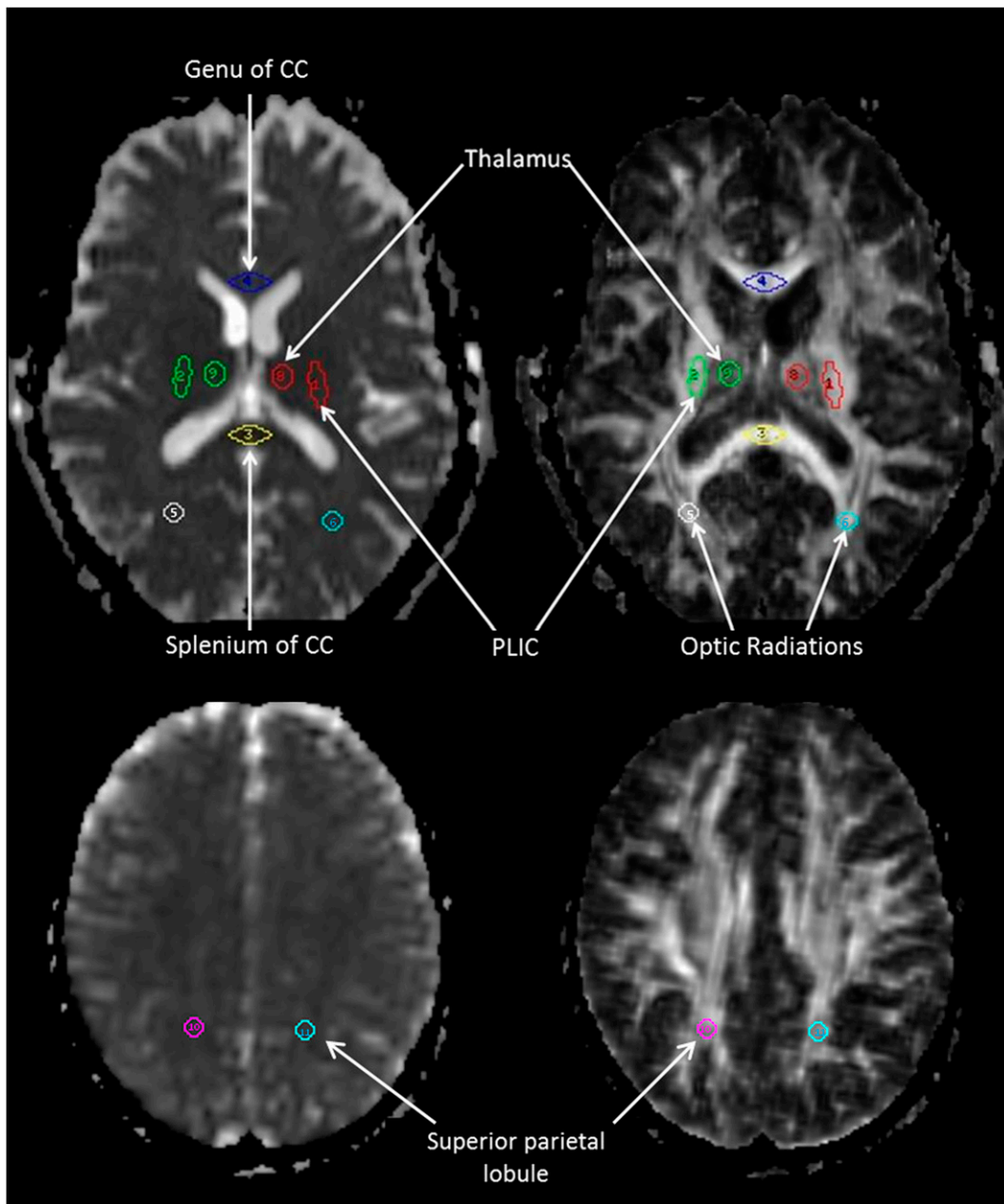


FIG. 1. ROIs defined on a T2 (*left*) and fractional anisotropy (*right*) image. CC, corpus callosum; PLIC, posterior limb of the internal capsule. (A high-quality color representation of this figure is available in the online issue.)

( $\chi^2 = 17.95$ ,  $P < 0.001$ ; Table 2). None of the T1DM patients had a history of retinopathy or neuropathy.

**ROI analyses.** Fractional anisotropy was lower ( $F_{1,99} = 7.59$ ,  $P = 0.007$ ) and radial diffusivity was higher ( $F_{1,99} = 7.45$ ,  $P = 0.008$ ) in the T1DM group compared with control subjects in the superior parietal lobule region. No differences were seen between groups in the hippocampus (fractional anisotropy, mean, radial, and axial diffusivities; Table 3). For exploratory regions, the T1DM group had lower mean ( $F_{1,99} = 10.36$ ,  $P = 0.002$ ) and lower radial diffusivity ( $F_{1,99} = 9.37$ ,  $P = 0.003$ ) in the thalamus and lower axial diffusivity in the cerebellum ( $F_{1,99} = 9.08$ ,  $P = 0.003$ ) compared with control subjects (Table 3).

**TBSS.** The T1DM group had lower axial diffusivity across multiple regions, including the superior parietal lobule, corpus callosum (genu, body, and splenium), posterior

limb of the internal capsule, external capsule, and cerebral peduncle, compared with controls (Fig. 2A). There were no differences in fractional anisotropy, mean diffusivity, or radial diffusivity parametric maps between the two groups.

#### Hyperglycemia categories

**Demographic and clinical data.** Subjects in the three hyperglycemia categories (0, 1–2, 3+) were similar in all of the demographic and clinical measures collected, with the exception that there were significantly fewer Caucasians in the 3+ group ( $\chi^2 = 9.79$ ,  $P = 0.008$ ; Table 2).

**ROI analyses.** The superior parietal lobule had decreased fractional anisotropy ( $F_{5,97} = 2.88$ ,  $P = 0.005$ ) and increased radial diffusivity ( $F_{5,97} = 2.99$ ,  $P = 0.009$ ) with increased hyperglycemic episodes. The 3+ hyper patients had the lowest fractional anisotropy (3+ hyper less than control subjects,  $P = 0.009$ ) and the highest radial

TABLE 2  
Demographic and clinical variables

	Control subjects N = 30	T1DM subjects N = 73	Among T1DM group (n = 73)					
			Severe hyper episodes			Severe hypo episodes		
			None n = 41	1-2 n = 21	3+ n = 11	None n = 27	1-2 n = 30	3+ n = 16
Age, years (SD)	15.9 (3.4)	16.8 (2.9)	16.9 (2.8)	16.2 (3.3)	17.4 (2.5)	16.6 (3.0)	16.7 (2.7)	17.1 (3.4)
Sex, n (% female)	15 (50)	29 (40)	17 (41)	8 (38)	4 (36)	8 (30)	14 (47)	7 (44)
Race, n (% Caucasian)†	27 (90)	65 (90)	37 (90)	21 (100)	7 (64)†	25 (93)	27 (90)	13 (81)
Handedness, n (% right handed)**	29 (97)	63 (86)**	35 (85)	20 (95)	8 (73)	23 (85)	26 (87)	14 (88)
Parental education, years (SD)	15.4 (1.9)	15.2 (2.1)	15.3 (2.3)	15.2 (1.6)	14.7 (1.7)	14.4 (1.9)	15.7 (2.0)	15.3 (2.1)
T1DM duration, years (SD)§	NA	9.5 (2.9)	9.1 (2.6)	9.9 (3.5)	9.9 (3.1)	7.9 (2.2)§	10.2 (3.0)	10.6 (2.9)
Age of T1DM onset, years (SD)‡	NA	7.2 (3.1)	7.8 (3.4)	6.1 (2.6)	7.5 (2.6)	8.5 (3.2)‡	6.5 (2.9)	6.5 (3.0)
HbA <sub>1c</sub> , median (SD)*	NA	8.3 (1.0)	8.2 (0.8)	8.2 (1.0)	9.1 (1.4)	8.3 (1.0)	8.1 (0.7)	9 (1.3)*
Weighted HbA <sub>1c</sub> , mean (SD)#	NA	-0.04 (1.3)	-0.26 (1.2)	-0.04 (1.4)	0.87 (1.3)	-0.63 (1.08)	-0.02 (1.14)	0.91 (1.64)#
Blood glucose at time of scan, mean mg/dL (SD)	NA	193.44 (91.8)	207.1 (89.6)	173.5 (96.8)	180 (90.0)	193.9 (89.1)	173 (83.1)	233.5 (104.9)

\*\*P < 0.001, #P = 0.03 significantly different among T1DM subjects; †P = 0.008; ‡P = 0.037; §P = 0.002; \*P = 0.04.

diffusivity (3+ hyper greater than controls, P = 0.013). We also found that increased hyperglycemic episodes were associated with higher mean (F<sub>5,97</sub> = 2.64, P = 0.034) and higher radial diffusivity (F<sub>5,97</sub> = 3.02, P = 0.034) in the hippocampus, with the 3+ hyper patients having the highest mean (3+ greater than 1-2 hyper, P = 0.043) and highest radial diffusivity (3+ greater than 1-2 hyper, P = 0.052). None of the exploratory regions were statistically different among the three hyperglycemic categories and the control group.

**TBSS.** One-way ANOVA identified significantly different axial diffusivity values along multiple white matter tracts, including the posterior limb of the internal capsule, external capsule, and cerebral peduncle, between the different hyperglycemic groups; however, none of the pairwise comparisons reached our predesignated statistical significance (Fig. 2B). There were no differences in fractional anisotropy, mean diffusivity, or radial diffusivity parametric maps among the hyperglycemic groups and controls.

**Hypoglycemia categories**

**Demographic and clinical data.** Subjects in the three hypoglycemia categories were similar in all demographic measures collected. In clinical measures, youth in the different hypoglycemic groups differed in age of onset (F<sub>2,72</sub> = 3.46, P = 0.037), median HbA<sub>1c</sub> (F<sub>2,63</sub> = 3.4, P = 0.04), and duration of disease (F<sub>2,71</sub> = 6.82, P = 0.002), with the 3+ hypo group having higher median HbA<sub>1c</sub> (3+ higher than 1-2 hypo group, P = 0.037), and those who experienced a severe hypoglycemic episode having longer duration of disease (0 shorter than 1-2 hypo group, P = 0.007; 0 shorter than 3+ hypo group, P = 0.007; Table 2).

**ROI analyses.** We found that the superior parietal lobule exhibited increased fractional anisotropy (F<sub>5,97</sub> = 2.97, P = 0.045) with increased hypoglycemic episodes, but none of the pairwise comparisons were significant. No differences

were found among the different groups in the DTI measures of the hippocampus. In addition, none of the exploratory regions were statistically significantly different among the hypoglycemic categories.

**TBSS.** One-way ANOVA identified significantly different axial diffusivity values along multiple white matter tracts, including the superior posterior limb of the internal capsule, external capsule, and cerebral peduncle, between the different hypoglycemic groups, but none of the pairwise comparisons reached significance (Fig. 2C). There were no differences in fractional anisotropy, mean diffusivity, or radial diffusivity parametric maps among the hypoglycemic groups and control subjects.

**Hyperglycemia score.** Our ROI-based DTI measures showed that none of the regions exhibited a statistically significant correlation between their fractional anisotropy, or mean, radial, and axial diffusivity values and the hyperglycemia exposure score. Similarly, using the TBSS approach, we did not find a significant correlation between hyperglycemia exposure score and the fractional anisotropy or mean, radial, and axial diffusivity parametric maps.

**DISCUSSION**

In this study, we detected differences in white and gray matter microstructure between youth with T1DM and their nondiabetic siblings using ROI and voxel-based analyses of diffusion tensor images. These findings suggest that DTI is a sensitive method for detecting brain abnormalities in T1DM, even in structures without apparent volumetric changes on conventional MRI.

Previous work from our laboratory and others has found that greater hyperglycemic exposure within the T1DM group was associated with reduced white and gray matter volume in the superior parietal lobule, particularly the

TABLE 3  
T1DM versus nondiabetic sibling control youth

	Fractional anisotropy (dimensionless)		Effect size (Cohen's <i>d</i> )	Mean diffusivity (mm/s)		Effect size (Cohen's <i>d</i> )	Radial diffusivity (mm/s)		Effect size (Cohen's <i>d</i> )	Axial diffusivity (mm/s)		Effect size (Cohen's <i>d</i> )
	Control subjects	T1DM subjects		Control subjects	T1DM subjects		Control subjects	T1DM subjects		Control subjects	T1DM subjects	
A priori regions												
Superior parietal lobule	0.465 ± 0.05	0.435 ± 0.05*	0.60	0.743 ± 0.02	0.747 ± 0.03	0.16	0.540 ± 0.04	0.562 ± 0.04*	0.55	1.149 ± 0.07	1.118 ± 0.07	0.44
Hippocampus	0.149 ± 0.02	0.153 ± 0.03	0.16	0.899 ± 0.06	0.883 ± 0.09	0.21	0.827 ± 0.05	0.812 ± 0.07	0.25	1.034 ± 0.08	1.022 ± 0.11	0.12
Exploratory regions												
Posterior limb of the internal capsule	0.590 ± 0.02	0.585 ± 0.03	0.20	0.673 ± 0.01	0.667 ± 0.01	0.60	0.417 ± 0.02	0.417 ± 0.02	0.00	1.186 ± 0.03	1.168 ± 0.04	0.51
Corpus callosum												
Splenium	0.791 ± 0.03	0.787 ± 0.04	0.11	0.663 ± 0.03	0.653 ± 0.05	0.24	0.266 ± 0.03	0.266 ± 0.05	0.00	1.458 ± 0.07	1.427 ± 0.09	0.38
Genu	0.715 ± 0.05	0.712 ± 0.04	0.07	0.705 ± 0.05	0.694 ± 0.04	0.24	0.349 ± 0.06	0.346 ± 0.05	0.05	1.416 ± 0.06	1.391 ± 0.06	0.42
Body	0.590 ± 0.06	0.592 ± 0.07	0.03	0.784 ± 0.06	0.772 ± 0.08	0.17	0.486 ± 0.08	0.478 ± 0.10	0.09	1.380 ± 0.06	1.360 ± 0.07	0.31
Optic radiation	0.516 ± 0.04	0.506 ± 0.04	0.25	0.759 ± 0.04	0.762 ± 0.04	0.08	0.514 ± 0.04	0.522 ± 0.04	0.20	1.249 ± 0.05	1.241 ± 0.05	0.16
Centrum semiovale	0.397 ± 0.04	0.382 ± 0.03	0.42	0.693 ± 0.02	0.691 ± 0.02	0.10	0.538 ± 0.03	0.547 ± 0.02	0.35	1.003 ± 0.05	0.983 ± 0.04	0.44
Thalamus	0.272 ± 0.01	0.279 ± 0.02	0.44	0.751 ± 0.02	0.736 ± 0.02**	0.75	0.643 ± 0.02	0.627 ± 0.02**	0.80	0.966 ± 0.03	0.955 ± 0.02	0.43
Putamen	0.114 ± 0.02	0.112 ± 0.02	0.10	0.714 ± 0.02	0.705 ± 0.02	0.45	0.675 ± 0.02	0.667 ± 0.02	0.40	0.793 ± 0.02	0.780 ± 0.02	0.65
Cerebellum	0.230 ± 0.04	0.219 ± 0.03	0.31	0.692 ± 0.03	0.683 ± 0.02	0.35	0.611 ± 0.04	0.607 ± 0.03	0.11	0.855 ± 0.03	0.835 ± 0.03***	0.67
Pons	0.399 ± 0.04	0.407 ± 0.05	0.18	0.668 ± 0.03	0.657 ± 0.03	0.37	0.511 ± 0.03	0.499 ± 0.04	0.34	0.982 ± 0.05	0.973 ± 0.06	0.16

Data are presented as mean ± SD. \**P* < 0.01, \*\**P* < 0.005.

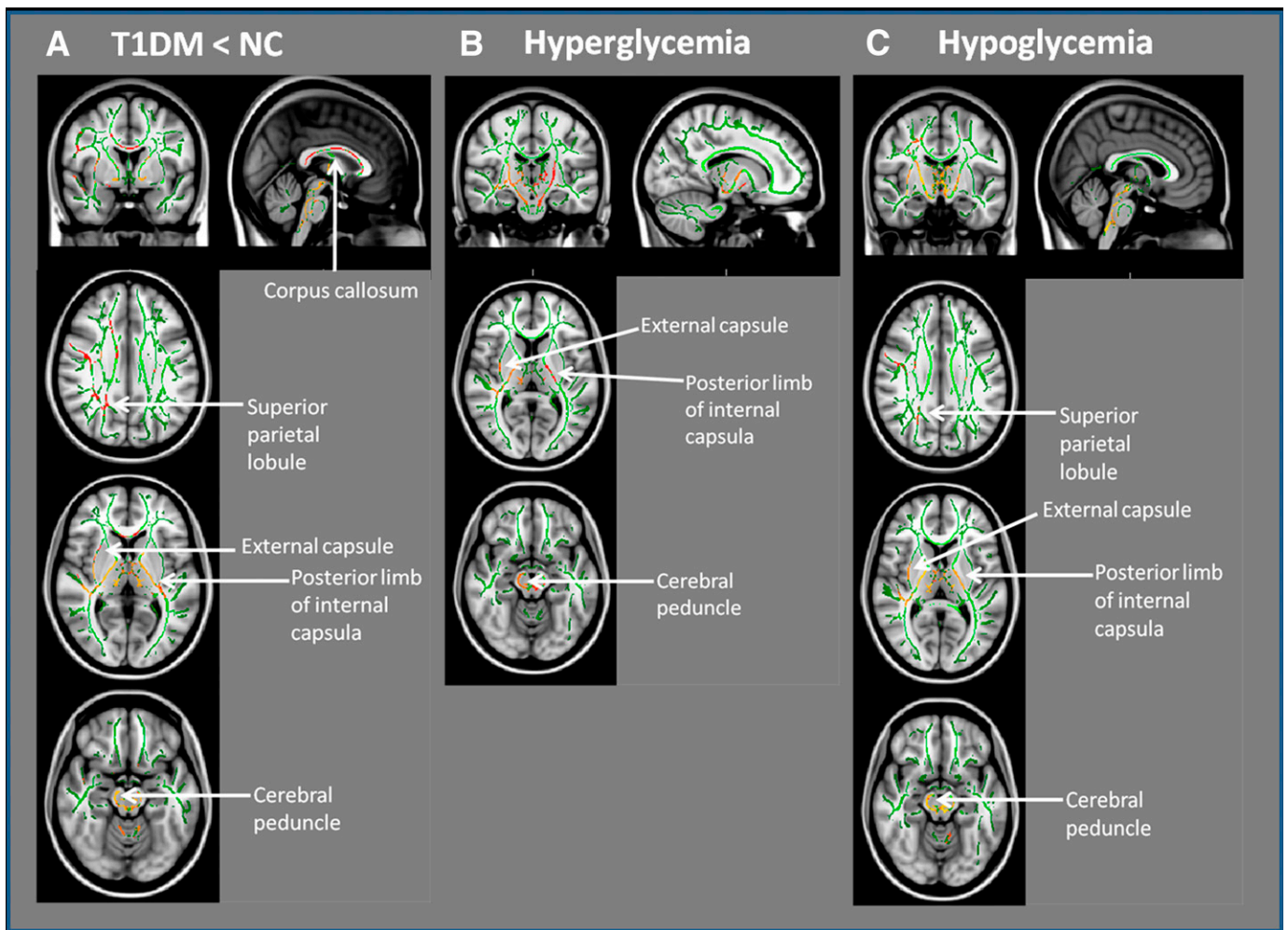


**FIG. 2.** *A:* TBSS results comparing axial diffusivity maps between T1DM and control subjects, which were reduced in T1DM youth compared with control subjects. *B:* Different severe hyperglycemic categories and control subjects. One-way ANOVA was significant, but none of the pairwise comparisons reached significance. *C:* Severe hypoglycemic categories and control subjects. One-way ANOVA was significant, but none of the pairwise comparisons reached significance. Green, TBSS skeleton; red,  $P = 0.05$ ; orange,  $P = 0.02$ . (A high-quality digital representation of this figure is available in the online issue.)

precuneus/cuneus cortical region (4–6). In the current study, we consistently observed that T1DM had altered DTI parameters in this region compared with controls, even after controlling for age and sex. Furthermore, DTI measures were particularly altered in the T1DM subjects in the 3+ hyper group, which suggests that this brain region may be an area of preferential sensitivity to hyperglycemia in T1DM. Hyperglycemia could affect white or gray matter integrity in the brain through several mechanisms, including mitochondrial superoxide production (23). Animal studies have found that hyperglycemia causes alterations in mitochondrial dynamics and function (24), which leads to accumulation of reactive oxygen species, oxidative stress, and impaired axonal transport in central nervous system axons, which can then result in axonal degeneration (25). This mechanism could provide some rationale why the superior parietal lobule, which is located within the precuneus/cuneus cortical region, appears particularly vulnerable to hyperglycemia. The precuneus/cuneus region is known to have the highest levels of glycolysis in the brain in resting state conditions (26). A high rate of glycolytic activity due to systemic hyperglycemia could possibly make brain tissue more vulnerable to damage or dysfunction by augmenting a metabolism-

dependent cascade such as hyperglycemia-induced oxidative stress (25,27). Alternatively, the DTI changes reported here could also be due to other glycolysis-independent biological factors that are altered concurrently with severe hyperglycemic episodes.

The pattern of DTI alterations can provide clues to the underlying neuropathology in the brain. Animal studies suggest that the combination of decreased fractional anisotropy, increased radial diffusivity, and decreased axial diffusivity is indicative of acute axonal injury along white matter tracts (14,28). In contrast, increased radial diffusivity, without an accompanying decrease in fractional anisotropy, is consistent with demyelinated white matter tracts (28). Thus, the pattern of differences in DTI parameters detected in the superior parietal lobule in particular, and across the brain using TBSS, is suggestive of axonal injury as opposed to demyelination of axons.

Although DTI traditionally is used to characterize white matter, DTI can also be used to examine mean diffusivity in gray matter regions, including the thalamus, putamen, and globus pallidus (29). Our a priori ROI for gray matter was the hippocampus, due to the extensive literature linking hyperglycemia and hypoglycemia exposure to changes in this region (30–34). We found that T1DM youth

exhibited increased mean and radial diffusivity in the hippocampus that was associated with hyperglycemic exposure. Our earlier work demonstrated that greater exposure to severe hypoglycemia, but not hyperglycemia, was associated with larger hippocampal volumes in T1DM youth. These seemingly disparate results emphasize that DTI and volumetric analyses examine complementary, but different, characteristics of brain structure, yet both point to significant alterations in the hippocampus in diabetes.

Among our exploratory regions, we found reduced diffusivity in the thalamus of T1DM youth. This finding is notable because the thalamus has also been associated with T1DM and glycemic exposure in other imaging and neuropathological studies of adults (35–37) and youth (1). Specifically, diabetic ketoacidosis has been reported to acutely affect the diffusivity of the thalamus in a pediatric population (38,39). Our findings suggest that the thalamus may exhibit long-term consequences associated with multiple diabetic ketoacidosis episodes. Differences in the diffusivity of these gray matter regions could reflect direct pathologic damage or secondary degeneration due to the disruption of white matter tracts linking these structures to other areas (29).

Our study is strengthened by a relatively large sample size and complementary DTI analyses strategies with good control of type I error. There is some overlap between our ROI-based and TBSS findings (Table 4), such as identification of the superior parietal lobule as a preferentially affected region in T1DM youth. Some ROIs, such as the thalamus, cannot be investigated using TBSS due to its limitation to white matter tracts. However, we did not

identify the external capsule as an exploratory region but saw differences in the axial diffusivity of this white matter tract using TBSS. We also note that the average effect sizes of the fractional anisotropy, mean, and radial diffusivity values obtained using our ROI-based approach are smaller compared with the average effect size of the axial diffusivity measures (Table 3). This may account for our ability to find significant differences between our study groups in the axial diffusivity parametric maps only using TBSS (Table 4).

Our results differ from the DTI findings in adults with T1DM. Although T1DM adults had lower fractional anisotropy than control subjects in the posterior corona radiata and the optic radiation (40) that correlated with hyperglycemic exposure (41), these results were not confirmed in our cohort of youth with T1DM. These differences could be due to the longer disease duration and/or greater degree of exposure to hyperglycemia in T1DM adults compared with our youth cohort and underscores the necessity of conducting separate neuroimaging studies during development. We also cannot rule out that the DTI differences reported here were present before exposure to glycemic extremes or diabetes. Retrospective report of severe glycemic experiences has been found to be fairly reliable (42), but prospective measures are likely to be more accurate, especially over long periods of time (43). Analysis of the prospective follow-up data from our study population is ongoing and should be able to determine if further exposure to hyperglycemia accentuates the DTI differences reported here. Finally, the current study cannot discern whether severe hyperglycemia itself, or factors that occur concurrently with severe hyperglycemic

TABLE 4  
Summary of analysis and results

Contrasts	Analysis	FA	MD	RD	AD
T1DM vs. NC	ROI	Superior parietal lobule (NC > T1DM) <i>P</i> = 0.007	Thalamus (NC > T1DM) <i>P</i> = 0.002	Superior parietal lobule (NC < T1DM) <i>P</i> = 0.008 Thalamus (NC > T1DM) <i>P</i> = 0.003	Cerebellum (NC > T1DM) <i>P</i> = 0.003
	TBSS	NS	NS	NS	Multiple significant regions (NC > T1DM)
Severe hyperglycemia categories	ROI	Superior parietal lobule (NC > 3+) <i>P</i> = 0.005	Hippocampus (1–2 < 3+) <i>P</i> = 0.034	Superior parietal lobule (NC < 3+) <i>P</i> = 0.009 Hippocampus (1–2 < 3+) <i>P</i> = 0.034	NS
	TBSS	NS	NS	NS	Multiple significant regions (NC > T1DM)
Severe hypoglycemia categories	ROI	Superior parietal lobule (1–2 < 3+) <i>P</i> = 0.045	NS	NS	NS
	TBSS	NS	NS	NS	Multiple significant regions (NC > T1DM)
Hyperglycemia exposure score	ROI	NS	NS	NS	NS
	TBSS	NS	NS	NS	NS

AD, axial diffusivity; FA, fractional anisotropy; MD, mean diffusivity; NC, normal control subjects; RD, radial diffusivity.

episodes, are more closely associated to the alterations in DTI measures we report in this study.

We conclude that youth with type 1 diabetes exhibit a pattern of regional DTI differences that is suggestive of axonal injury or degeneration, some of which may be related to severe hyperglycemic exposure. Longitudinal follow-up of well-characterized samples such as ours will be critical in determining the course of brain changes with age and further exposure to glycemic extremes. Finally, an understanding of the implications of these findings for optimal cognitive and academic function must be obtained to place these observations in proper clinical context.

#### ACKNOWLEDGMENTS

This work was supported by the Dana Foundation and the National Institutes of Health (grant numbers DK-64832, 5T32-DA-007261-20 and UL1-RR-024992).

No potential conflicts of interest relevant to this article were reported.

J.A.V.A.-D. and T.H. researched data, contributed to discussions, and wrote, reviewed, and edited the manuscript. E.M. researched data, contributed to discussions, and reviewed and edited the manuscript. J.R. researched data, contributed to discussions, and reviewed the manuscript. D.C.P. researched data and reviewed and edited the manuscript. N.H.W., A.M.A., and J.S.S. contributed to discussions and reviewed and edited the manuscript. J.A.V.A.-D. and T.H. are the guarantors of this work, and, as such, had full access to all the data and take full responsibility for the integrity of data and the accuracy of data analysis.

The authors thank the participants and their families for their support. The authors also thank (all from the Department of Psychiatry, Washington University) Jenny Wu, Aiden Bondurant, and Patrick Weaver for assistance in study recruitment and data analysis and Heather Lugar for help in scanning subjects.

The data in this article were presented at the 72nd Scientific Sessions of the American Diabetes Association Philadelphia, Pennsylvania, 8–12 June 2012.

#### REFERENCES

- Northam EA, Rankins D, Lin A, et al. Central nervous system function in youth with type 1 diabetes 12 years after disease onset. *Diabetes Care* 2009;32:445–450
- Aye T, Reiss AL, Kesler S, et al. The feasibility of detecting neuro-psychologic and neuroanatomic effects of type 1 diabetes in young children. *Diabetes Care* 2011;34:1458–1462
- Perantie DC, Koller JM, Weaver PM, et al. Prospectively determined impact of type 1 diabetes on brain volume during development. *Diabetes* 2011;60:3006–3014
- Perantie DC, Wu J, Koller JM, et al. Regional brain volume differences associated with hyperglycemia and severe hypoglycemia in youth with type 1 diabetes. *Diabetes Care* 2007;30:2331–2337
- Musen G, Lyoo KL, Sparks C, et al. Evidence for reduced gray matter density in patients with type 1 diabetes as measured by magnetic resonance imaging. *Diabetes* 2004;52(Suppl. 2):A57–A58
- Wessels AM, Simsek S, Remijnse PL, et al. Voxel-based morphometry demonstrates reduced grey matter density on brain MRI in patients with diabetic retinopathy. *Diabetologia* 2006;49:2474–2480
- Ho MS, Weller NJ, Ives FJ, et al. Prevalence of structural central nervous system abnormalities in early-onset type 1 diabetes mellitus. *J Pediatr* 2008;153:385–390
- Hershey T, Perantie DC, Wu J, Weaver PM, Black KJ, White NH. Hippocampal volumes in youth with type 1 diabetes. *Diabetes* 2010;59:236–241
- Sarac K, Alkinci A, Alkan A, Aslan M, Baysal T, Ozcan C. Brain metabolite changes on proton magnetic resonance spectroscopy in children with poorly controlled type 1 diabetes mellitus. *Neuroradiology* 2005;47:562–565
- Jamali R, Mohseni S. Differential neuropathies in hyperglycemic and hypoglycemic diabetic rats. *J Neuropathol Exp Neurol* 2006;65:1118–1125
- Mohseni S. Hypoglycemic neuropathy. *Acta Neuropathol* 2001;102:413–421
- Mac Donald CL, Johnson AM, Cooper D, et al. Detection of blast-related traumatic brain injury in U.S. military personnel. *N Engl J Med* 2011;364:2091–2100
- Shimony JS, Sheline YI, D'Angelo G, et al. Diffuse microstructural abnormalities of normal-appearing white matter in late life depression: a diffusion tensor imaging study. *Biol Psychiatry* 2009;66:245–252
- Budde MD, Xie M, Cross AH, Song SK. Axial diffusivity is the primary correlate of axonal injury in the experimental autoimmune encephalomyelitis spinal cord: a quantitative pixelwise analysis. *J Neurosci* 2009;29:2805–2813
- Hershey T, Perantie DC, Warren SL, Zimmerman EC, Sadler M, White NH. Frequency and timing of severe hypoglycemia affects spatial memory in children with type 1 diabetes. *Diabetes Care* 2005;28:2372–2377
- Perantie DC, Lim A, Wu J, et al. Effects of prior hypoglycemia and hyperglycemia on cognition in children with type 1 diabetes mellitus. *Pediatr Diabetes* 2008;9:87–95
- The Diabetes Control and Complications Trial Research Group. The effect of intensive treatment of diabetes on the development and progression of long-term complications in insulin-dependent diabetes mellitus. *N Engl J Med* 1993;329:977–986
- The DCCT Research Group. Epidemiology of severe hypoglycemia in the diabetes control and complications trial. *Am J Med* 1991;90:450–459
- Oishi K, Zilles K, Amunts K, et al. Human brain white matter atlas: identification and assignment of common anatomical structures in superficial white matter. *Neuroimage* 2008;43:447–457
- Shimony JS, McKinstry RC, Akbudak E, et al. Quantitative diffusion-tensor anisotropy brain MR imaging: normative human data and anatomic analysis. *Radiology* 1999;212:770–784
- Smith SM, Jenkinson M, Johansen-Berg H, et al. Tract-based spatial statistics: voxelwise analysis of multi-subject diffusion data. *Neuroimage* 2006;31:1487–1505
- Nichols TE, Holmes AP. Nonparametric permutation tests for functional neuroimaging: a primer with examples. *Hum Brain Mapp* 2002;15:1–25
- Brownlee M. The pathobiology of diabetic complications: a unifying mechanism. *Diabetes* 2005;54:1615–1625
- Vincent AM, Edwards JL, McLean LL, et al. Mitochondrial biogenesis and fission in axons in cell culture and animal models of diabetic neuropathy. *Acta Neuropathol* 2010;120:477–489
- Sharma R, Buras E, Terashima T, et al. Hyperglycemia induces oxidative stress and impairs axonal transport rates in mice. *PLoS ONE* 2010;5:e13463
- Vaishnavi SN, Vlassenko AG, Rundle MM, Snyder AZ, Mintun MA, Raichle ME. Regional aerobic glycolysis in the human brain. *Proc Natl Acad Sci USA* 2010;107:17757–17762
- Vincent AM, Brownlee M, Russell JW. Oxidative stress and programmed cell death in diabetic neuropathy. *Ann N Y Acad Sci* 2002;959:368–383
- Zhang J. Diffusion tensor imaging of white matter pathology in the mouse brain. *Imaging Med* 2010;2:623–632
- O'Sullivan M, Singhal S, Charlton R, Markus HS. Diffusion tensor imaging of thalamus correlates with cognition in CADASIL without dementia. *Neurology* 2004;62:702–707
- Auer RN, Hugh J, Cosgrove E, Curry B. Neuropathologic findings in three cases of profound hypoglycemia. *Clin Neuropathol* 1989;8:63–68
- Malone JJ, Hanna S, Saporta S, et al. Hyperglycemia not hypoglycemia alters neuronal dendrites and impairs spatial memory. *Pediatr Diabetes* 2008;9:531–539
- Chalmers J, Risk MTA, Kean DM, Grant R, Ashworth B, Campbell IW. Severe amnesia after hypoglycemia. Clinical, psychometric, and magnetic resonance imaging correlations. *Diabetes Care* 1991;14:922–925
- Kalimo H, Olsson Y. Effects of severe hypoglycemia on the human brain. Neuropathological case reports. *Acta Neurol Scand* 1980;62:345–356
- Gold SM, Dziobek I, Sweat V, et al. Hippocampal damage and memory impairments as possible early brain complications of type 2 diabetes. *Diabetologia* 2007;50:711–719
- Ohara S, Nakagawa S, Tabata K, Hashimoto T. Hemiballism with hyperglycemia and striatal T1-MRI hyperintensity: an autopsy report. *Mov Disord* 2001;16:521–525
- Musen G, Lyoo IK, Sparks CR, et al. Effects of type 1 diabetes on gray matter density as measured by voxel-based morphometry. *Diabetes* 2006;55:326–333
- Postuma RB, Lang AE. Hemiballism: revisiting a classic disorder. *Lancet Neurol* 2003;2:661–668



38. Glaser NS, Marcin JP, Wootton-Gorges SL, et al. Correlation of clinical and biochemical findings with diabetic ketoacidosis-related cerebral edema in children using magnetic resonance diffusion-weighted imaging. *J Pediatr* 2008;153:541–546
39. Vavilala MS, Marro KI, Richards TL, et al. Change in mean transit time, apparent diffusion coefficient, and cerebral blood volume during pediatric diabetic ketoacidosis treatment. *Pediatr Crit Care Med* 2011;12:e344–e349
40. van Duinkerken E, Schoonheim MM, Ijzerman RG, et al. Diffusion tensor imaging in type 1 diabetes: decreased white matter integrity relates to cognitive functions. *Diabetologia* 2012;55:1218–1220
41. Kodl CT, Franc DT, Rao JP, et al. Diffusion tensor imaging identifies deficits in white matter microstructure in subjects with type 1 diabetes that correlate with reduced neurocognitive function. *Diabetes* 2008;57:3083–3089
42. Deary IJ, Langan SJ, Graham KS, Hepburn DA, Frier BM. Recurrent severe hypoglycemia, intelligence, and speed of information processing. *Intelligence* 1992;16:337–359
43. Gold AE, MacLeod KM, Frier BM. Frequency of severe hypoglycemia in patients with type 1 diabetes with impaired awareness of hypoglycemia. *Diabetes Care* 1994;17:697–703